UNIVERSITY OF
BATH

University of Bath

Alternative formats
If you require this document in an alternative format, please contact:
openaccess@bath.ac.uk

Effect of Anionic Lipids on Ion Permeation through the KcsA K+-Channel

Victoria Oakes[1], Simone Furini[2] and Carmen Domene[1,3]

[1]Department of Chemistry, University of Bath, Claverton Down, Bath, BA2 7AY, UK
[2]Department of Medical Biotechnologies, University of Siena, Siena, Italy
[3]Department of Chemistry, University of Oxford, Oxford, OX1 3TA, UK

Abstract

K^+-channels are responsible for the efficient and selective conduction of K^+ ions across the plasma membrane. The bacterial K^+ channel KcsA has historically been used to characterize various aspects of K^+ conduction via computational means. The energetic barriers associated with ion translocation across the KcsA selectivity filter have been computed in various studies, leading to the proposal of two alternate mechanisms of conduction, involving or neglecting the presence of water molecules in between the permeating ions. Here, the potential of mean force of K^+ permeation is evaluated for KcsA in lipid bilayers containing anionic lipids, which is known to increase the open probability of the channel. In addition, the effect of the protonation/deprotonation of residue E71, which directly interacts with the selectivity filter sequence, is assessed. Both conduction mechanisms are considered throughout. The results obtained provide novel insights into the molecular functioning of K^+ channels including the inactivation process.

Keywords: molecular dynamics simulations; umbrella sampling; conduction mechanism; cell membrane; lipid-protein interactions

Introduction

The plasma membrane is a critical regulator of ion channel function. Various membrane lipids have been shown to exert an effect on ion channels from a diverse range of families, including cholesterol, and several types of phospholipids (such as phosphatidylinositol 4,5-bisphosphate) and sphingolipids (such as sphingosine-2-phosphate) [1-3]. Membrane lipids can regulate ion channel activity by several mechanisms among which are: (i) direct binding to specific sites on the channel surface, (ii) perturbation of the physical properties of the phospholipid bilayer, and (iii) modulation of complex formation with other protein assemblies. In the K^+-channel family, the regulation of several channel types by membrane lipids has been investigated, including inward-rectifying and voltage-gated K^+-channels [1, 4, 5]. In KcsA, a bacterial K^+-channel, it has been shown that anionic phospholipids are instrumental to channel function. For instance, the conductance and open probability of KcsA increases in the presence of anionic lipids [6, 7] Moreover, anionic lipids enhance the structural stability of KcsA, in conditions of thermal or chemical denaturation [8-10]. In addition, correct folding *in vitro* is assisted by anionic lipids [11]. However, the exact role of anionic lipids in these processes remains unclear.

The landmark crystal structure of KcsA revealed the structure of the K^+-channel pore domain in atomic detail [12]. The homotetramer is formed from the assembly of four identical subunits, each containing two transmembrane helices, connected by a loop which converges at the center of the channel (Figure 1). The pore-loop, as this is known, contains an α-helix and the selectivity filter sequence (TVGYG), which is conserved in prokaryotic and eukaryotic K^+-channels [13, 14]. This region is responsible for permitting fast and efficient permeation of K^+ ions, whilst excluding other ionic species. A symmetric arrangement of the backbone carbonyl groups of the selectivity filter sequence and the sidechain of the included threonine form four adjacent binding sites, named S1-S4, which can accommodate dehydrated K^+ ions (Figure 2A). Ions enter from the cytoplasm to a water-filled cavity in the center of the protein, and then penetrate the selectivity filter before exiting to the periplasm. Numerous computational studies have been devoted to conduction in K^+-channels [15-20] . On the base of molecular dynamics (MD) simulations, two alternative mechanisms were proposed for ion movements across the selectivity filter, referred here as KWK and KK [21]. In the KWK mechanism, two consecutive ions in the selectivity filter are separated by an intervening water molecule, while in the KK mechanism, the filter is completely depleted from water molecules, and ions occupy consecutive sites or are separated by empty sites. Ion conduction is regulated at the lower gate by opening and closing of the transmembrane helices, and at the upper gate by activation and

inactivation of the selectivity filter. It is, therefore, possible that anionic lipids can act at two distinct sites to modulate ion conductance in KcsA.

Several clues into the mechanism of lipid regulation have been gained from the abundance of high-resolution structural information available for the KcsA channel. Re-examination of an early KcsA structure has disclosed the location of a binding site for anionic lipid POPG (1-palmitoyl-2-oleoyl-sn-glycero-3-phosphoglycerol), in a cleft at the interface between adjacent subunits, and in close proximity to the selectivity filter [22-24]. In these sites, typically referred to as 'non-annular sites' [25], several arginine residues are thought to be involved in the selective, high-affinity binding of phospholipids [4, 6, 26-28]. The behaviour of non-annular lipids has been directly implicated in the dynamics of selectivity filter residues [28, 29], providing a plausible mechanism of action of anionic lipids on the selectivity filter. Marius et al suggested that the inhabitance of three or four identical sites by anionic lipids is a prerequisite for channel opening [6]. What is more, the occupation of non-annular sites has been shown to encourage the formation of KcsA clusters, which exhibit altered conduction properties than isolated channels [30].

In this work, the energetics of ion conduction through the KcsA selectivity filter is evaluated using umbrella sampling simulations, in zwitterionic and mixed zwitterionic/anionic lipid bilayers. The potential of mean force is calculated when non-annular sites are unoccupied and occupied by both anionic and zwitterionic lipids. Although interaction between anionic lipids and the KcsA channel has been examined in several simulation studies [4, 28], none have systematically calculated conduction energetics in systems with anionic lipid components, providing the novel aspect to this work. This is supplemented by analogous calculations, where the protonation state of residues E71 is modified, which increases the negative charge density directly behind the selectivity filter and alters the conformation of proximal residues. The data obtained provides important insights into the molecular functioning of the selectivity filter in response to the introduction of anionic components.

Materials and Methods

Model Setup

Coordinates from the high-resolution crystal structure of KcsA in a closed state (PDB ID 1K4C), residues 26-114, were used to model the channel [31]. This particular structure was used to allow direct comparison with previous studies [21]. N- and C-termini were acetylated and methylated respectively. The amino acid E71 of KcsA was modelled in the protonated

state to form a diacid hydrogen bond with D80 [32]. Default ionisation states were used for the remaining amino acids. Four water molecules were placed at the back of the selectivity filter, in agreement with crystallographic data and previous MD simulations [23]. SOLVATE 1.0 was used to solvate internal cavities of the protein. The structures were aligned perpendicular to the bilayer and inserted into two membrane systems: (i) a neutral membrane containing 1-palmitoyl-2-oleoyl-sn-glycero-3-phosphocholine (POPC) molecules and (ii) a charged membrane constituted of POPC and 1-palmitoyl-2-oleoylphosphatidylserine (POPS) molecules in a 3:1 ratio, which were generated using the CHARMM-GUI online server [33-35]. Simulations where the protein is embedded in the POPC bilayer will be labelled POPC, and those where the protein is embedded in the mixed bilayer will be labelled POPS in what follows. The structures of POPC and POPS are shown in Figure 1B. The VMD solvate plugin was then used to create a cubic water box around the membrane-protein system [36]. The overlapping water and lipid molecules around the ion channel structure were removed with the cut-off distance 1.2 Å. Potassium and chloride ions were added using the Autoionize plugin of VMD to neutralize the systems up to a concentration of 150 mM [36]. The final system size was approximately 90,000 atoms; a representation of the system is shown in Figure 1A. Ions were initially placed in the S0, S2 and S4 positions, with water molecules in the remaining sites. The selectivity filter structure and the associated binding sites are defined in Figure 2. These simulations were denoted POPC/E71H/KWK and POPS/E71H/KWK (Table 1).
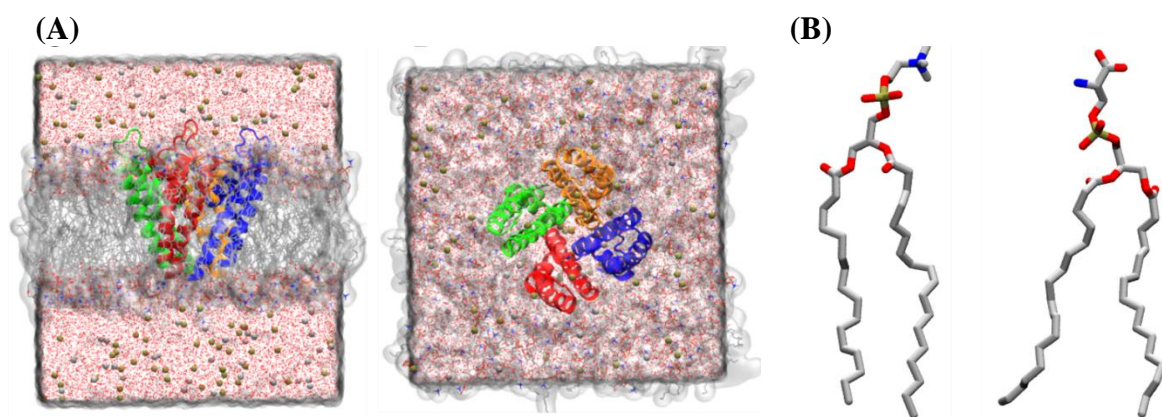
Figure 1. (A) Side and top view of a representative final simulation system. The protein is shown in cartoon representation, with individual subunits colored differently. Lipid molecules are shown in licorice representation, and K^+ and Cl^- ions are shown as white and ochre spheres, respectively. (B) Structure of POPC and POPS lipid molecules with carbon, oxygen, nitrogen and phosphorous atoms shown in grey, red, blue and gold, respectively.
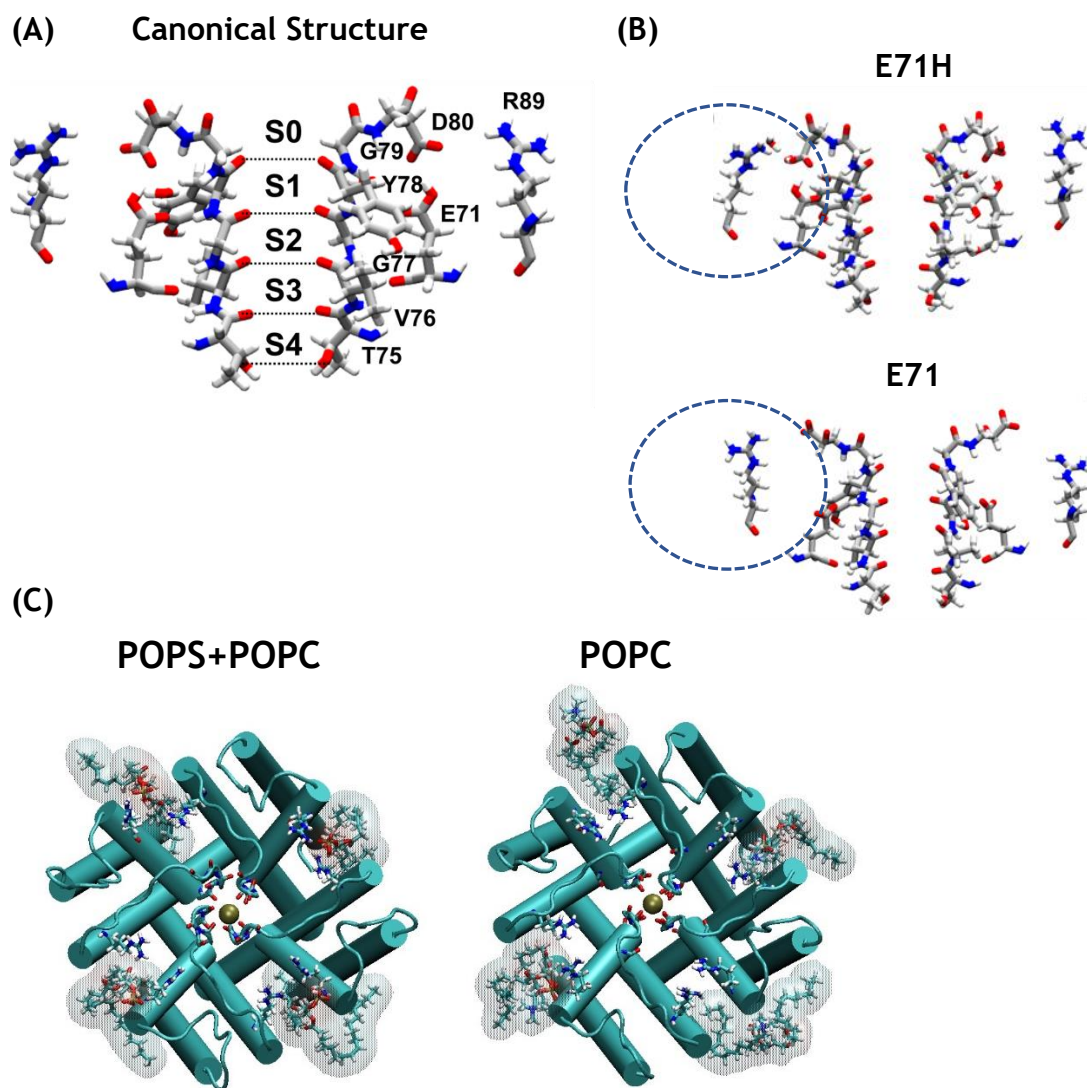
Figure 2. (A) Illustration of the structure of the KcsA selectivity filter in 'licorice' representation from the original crystal structure with binding sites labelled, along with relevant residues. **(B)** Representative structures of the selectivity filter of the systems considered are illustrated where the main difference lies in the presence of E71 protonated or not. Only two opposite subunits are shown for simplicity. KcsA is a homo-tetramer, and there are four identical non-annular sites, each of them acting on just one of the four sequence of Thr[75]-Val[76]-Gly[77]-Tyr[78]-Gly[79] residues from each subunit. This sequence contributes its carbonyl groups to configure the selectivity filter. **(C)** Two representative snapshots illustrating the protein-lipid interactions described in the main text in simulations with POPC-POPS or POPC-only membranes. Top view of the protein and non-annular sites occupied by POPS or POC lipids that interact with the protein. The protein backbone is shown in 'cartoon' in cyan. Atoms of two arginine side chains (R64 and R89) at the extracellular membrane side forms an electrostatic interaction with a POPS head group. These two Arg residues are shown in CPK representation, and the selectivity filter residues are shown in licorice representation. The lipid surfaces of non-annular POPS or POPC molecules are shown in licorice and Quicksurf representations superimposed. Potassium ions at the selectivity filter are represented by an ochre

sphere.

Molecular Dynamics Simulations

MD simulations were performed with NAMD version 2.12 [37]. CHARMM36 parameters were used for the protein and lipids [38], the TIP3P model was used for water [39]. Parameters for K^+ ions inside the selectivity filter were selected according to ref. [40]. Default CHARMM parameters were used for potassium ions in bulk solution and chloride ions. The particle mesh Ewald method was used for the treatment of periodic electrostatic interactions, with an upper threshold of 1 Å for grid spacing [41]. Electrostatic and van der Waals forces were calculated every time step. A cutoff distance of 12 Å was used for Van der Waals forces. A switching distance of 10 Å was chosen to smoothly truncate the non-bonded interactions. Only atoms in a Verlet pair list with a cutoff distance of 13.5 Å (reassigned every 20 steps) were considered. The SETTLE algorithm was used to constrain all bonds involving hydrogen atoms, to allow the use of a 2 fs time step throughout the simulation [42]. MD simulations were performed in the NPT ensemble. The Nose-Hoover-Langevin piston was employed to control the pressure with a 200 fs period, 50 fs damping constant, and the desired value of 1 atmosphere [43, 44]. The system was coupled to a Langevin thermostat to sustain a temperature of 300 K throughout. In the equilibration process, the same protocol was used for all the systems. The systems were subjected to 10,000 steps of minimization, with harmonic constraints (force constant 20 kcal $mol^{-1} Å^{-2}$) on protein atoms, lipid headgroups and crystallographic water and ions. Harmonic restraints were gradually reduced to a force constant of 2 kcal $mol^{-1} Å^{-2}$ and removed in consecutive steps from the lipid headgroups, protein sidechains and protein backbone over the course of a 3.5 ns trajectory. Initial 500 ns unbiased MD simulations (POPC/E71H/KWK and POPS/E71H/KWK) identified binding of charged and zwitterionic phospholipids in non-annular sites on the interface between two adjacent subunits. On account of this, analogous systems were then prepared by docking lipid molecules in the vacant sites, and new simulations were started from there after equilibration with full occupancy of the four non-annular binding sites ($POPC_4$/E71H/KWK and $POPS_4$/E71H/KWK) [6]. In other words, we had to artificially place lipid molecules in non-annular sites to set-up these other systems because their exchange time is much longer than the time-scale of the simulations we performed and lipid molecules did not spontaneously fil all the non-annular sites.

A representative snapshot illustrating the protein-POPS interactions in two out of the four non-annular sites is shown in Figure 2B. Additional unbiased simulations with residue E71 deprotonated were undertaken, with non-annular lipids present ($POPC_4$/E71/KWK and

POPS$_4$/E71/KWK). Coordinates from the first 50 ns of unconstrained MD simulations from these systems were used as the starting point for subsequent biased simulations, shown in Figure 2C. To prepare the equivalent simulations for the alternative conduction mechanism without water molecules separating the ions, the ions and water molecules in the selectivity filter were manually moved to the S1/S2/G/S4/S$_{CAV}$ configuration, where G is shorthand for gap, and S$_{CAV}$ indicates the intracellular cavity of the channel. S$_{EXT}$ refers to the ion at the extracellular side. A summary of the systems used for umbrella sampling is provided in Table 1.

Table 1. Summary of umbrella sampling simulations performed. W and G are shorthand for water and gap, respectively.

Bilayer Composition	E71 Protonation State	Non-Annular Lipids	Permeation Mechanism	Starting Configuration Ions in SF	Notation
POPC	Protonated	NO	KWK	S0/W/S2/W/S4/S$_{CAV}$	POPC/E71H/KWK
		NO	KK	S1/S2/G/S4/S$_{CAV}$	POPC/E71H/KK
		YES	KWK	S0/W/S2/W/S4/S$_{CAV}$	POPC$_4$/E71H/KWK
		YES	KK	S1/S2/G/S4/S$_{CAV}$	POPC$_4$/E71H/KK
	Deprotonated	YES	KWK	S0/W/S2/W/S4/S$_{CAV}$	POPC$_4$/E71/KWK
		YES	KK	S1/S2/G/S4/S$_{CAV}$	POPC$_4$/E71/KK
POPS+POPC	Protonated	NO	KWK	S0/W/S2/W/S4/S$_{CAV}$	POPS/E71H/KWK
		NO	KK	S1/S2/G/S4/S$_{CAV}$	POPS/E71H/KK
		YES	KWK	S0/W/S2/W/S4/S$_{CAV}$	POPS$_4$/E71H/KWK
		YES	KK	S1/S2/G/S4/S$_{CAV}$	POPS$_4$/E71H/KK
	Deprotonated	YES	KWK	S0/W/S2/W/S4/S$_{CAV}$	POPS$_4$/E71/KWK
		YES	KK	S1/S2/G/S4/S$_{CAV}$	POPS$_4$/E71/KK

Umbrella Sampling Simulations

The umbrella sampling technique has been widely used to calculate the Potential of Mean Force (PMF) of ion conduction in K$^+$-channels [21, 45-47]. Here, the technique has been employed to calculate the PMF of potassium ions translocation through the KcsA selectivity filter.

Considering the time scales associated with lipid exchanges, the times scales available to atomistic simulations, and the time scales associated to free energy simulations

Ion permeation involving four ions was examined. To simulate the KWK mechanism, where water molecules fill sites not containing K$^+$ ions, the events connecting the S0/S2/S4/S$_{CAV}$ and S$_{EXT}$/S0/S2/S4/ configurations were examined, with water molecules in remaining sites. To simulate the KK mechanism, where sites not containing K$^+$ ions are empty, the events connecting the S1/S2/S4/S$_{CAV}$ and S$_{EXT}$/S1/S2/S4/ were examined. As validated in previous studies [21], the initial and final configurations are considered to be equivalent. The ions

7

studied are denoted K1 (exterior ion), K2 (central ion 1), K3 (central ion 2) and K4 (interior ion). The position along the axis of K2 and K3 was controlled by a harmonic potential acting on the center of mass of the pair. The center of the biasing potential acting on K4 moved from the intracellular cavity to the binding site S4, while the biasing potential acting on K1 moved from the binding site S0 to the extracellular milieu. The position of the center of mass of the backbone oxygen atoms of the TVGY motif was chosen as reference. Individual simulations were predominantly spaced 1 Å apart, adopting a force constant of 10 kcal $mol^{-1}Å^{-2}$ for the harmonic potential. In the barrier regions, additional windows with a force constant of 20 kcal $mol^{-1}Å^{-2}$ for the harmonic potentials were used. In order to avoid degenerate states due to ions K2 and K3 switching positions with K1 and K4, simulations with alternative biasing potentials were added. In POPC$_4$/E71/KK, alternative biasing potentials acted upon the K1 ion, the K2 ion and the center of mass of both K3 and K4 ions. In POPS$_4$/E71/KK, alternative biasing potentials acted upon the K3 ion, the K4 ion and the center of mass of both K1 and K2 ions. At the start of each window, ions were manually moved to their starting configurations. Simulations of 500 ps were then performed for each configuration. The positions of water molecules in the selectivity filter were monitored throughout, and simulations exhibiting transitions between the KWK and KK mechanism were removed from subsequent analyses. The initial 100 ps of the trajectories were considered as equilibration, and also removed. The weighted histogram analysis method [48] was used to unbias the data and obtain the PMF in three or four (POPC$_4$/E71/KK and POPS$_4$/E71/KK) dimensions, which were then projected onto two-dimensions for visualization as previously described [21, 45-47]. The minimum energy path between the extreme ion configurations, that is, the energy barriers for the permeation process, was then computed on the 3-dimensional maps by the string method [49] as previously described [21]. Error estimates were obtained by calculating PMF profiles for 100-ps portions of the trajectory and combining them. These PMF profiles are representative of complete conduction events under the assumption that the entrance/exit of a K^+ ion to/from the intracellular cavity is not associated with large energetic barriers. In agreement with this hypothesis, the difference in solvation energy for a K^+ ion in the cavity or S$_{EXT}$, defined by the free energy difference between configuration (S$_{EXT}$/S0/S2/S$_4$) and (S0/S2/S4/S$_{CAV}$), is ≈1 kcal/mol in both mechanisms. Structural data [50] as well as electrostatics calculations [51] also support this hypothesis.

Results

Umbrella sampling simulations have been used to calculate the energetics of ion conduction through the KcsA selectivity filter. In the first section, three independent parameters have been modified in order to assess their effect: (i) ion permeation mechanism, either KK or KWK, (ii) membrane composition, and (iii) presence of non-annular lipids. The structure of the selectivity filter, with labelled binding sites, and the specific simulation frame used to seed the umbrella sampling simulations are shown in Figure 2, demonstrating the hydrogen-network. The results are organised by conduction mechanism to avoid repetition. In the following sections, the effect of deprotonating E71 is examined. Note that in the simplified representations of the selectivity filter shown along with the maps, only the ions at binding sites S0-S4 are explicitly depicted, while the remaining ion included in the PMF calculations at the intracellular/extracellular side of the selectivity filter is not considered. The consequence is that the free-energy of states identified by the same label might differ between the left and the right panels, because of the position of the fourth ion. The energy barriers were estimated using the full four-dimensional energy profiles.

KWK Mechanism

In the KWK mechanism of conduction, K^+ ions occupy non-adjacent sites in the selectivity filter *i.e.* S2/S4 or S1/S3, interspersed by water molecules. Ion transport occurs by concerted transitions between these configurations, associated with an incoming intracellular ion, and an outgoing extracellular ion. This has been supported experimental studies [52-54] and prior computational [15, 16, 21]. The PMFs corresponding to the KWK mechanism are shown in Figure 3A-D, and the estimated energetic barriers are reported in Table 2. When non-annular lipids are bound (POPS$_4$/E71H/KWK and POPC$_4$/E71H/KWK), an energetic cost of 3-4 kcal/mol is associated with loss of the exterior ion from S0 (transition I→II), as well as with the attachment of the cavity ion to the lower border of the S4 site (denoted S4$_B$ from this point forward) and the concurrent movement of selectivity filter ions from S2/S4 to S1/S3 (transition II→III). The subsequent ion movements to reform the S0/S2/S4 configuration poses the highest barrier to conduction, approximately of the order of 5 kcal/mol. The calculated barriers are consistent in POPS/E71H/KWK, albeit slightly higher in transition III→IV. In contrast, in POPC/E71H/KWK the barrier for transitions III→IV and II→III are elevated and decreased respectively. This difference can be attributed to alternate positions of the S1 ion in the S1/S3/S4$_B$ configuration: in POPC/E71H/KWK a pronounced well is seen in the center of the site, opposed to other simulations where the S1 and S1$_B$ positions (where S1$_B$ denotes the

lower border of the S1 site) are of equal energy (POPS$_4$/E71H/KWK and POPS/E71H/KWK) or the energy of S1$_B$ is slightly lower (POPC/E71H/KWK).

Table 2. Energetic barriers (>2 kcal/mol) calculated from umbrella sampling simulations for the KWK mechanism with residues E71 protonated (E71H).

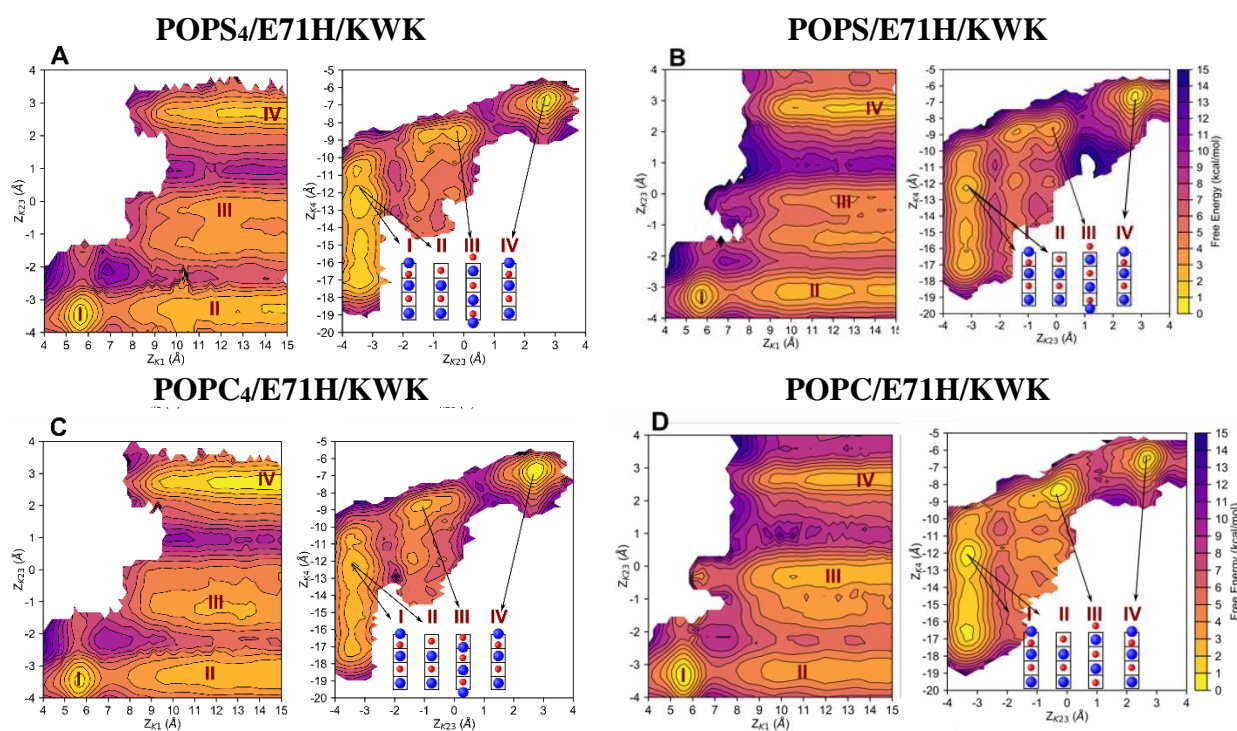| Simulation	Energy Barrier (kcal/mol ± SD)		
	I → II	II → III	III → IV
POPS$_4$/E71H/KWK	4.2 ± 0.6	3.6 ± 0.9	4.8 ± 1.2
POPS/E71H/KWK	3.4 ± 0.5	3.8 ± 0.7	6.7 ± 0.9
POPC$_4$/E71H/KWK	3.7 ± 0.8	3.3 ± 0.8	5.5 ± 0.9
POPC/E71H/KWK	5.5 ± 0.4	2.0 ± 0.6	6.7 ± 0.5

Figure 3. PMF profiles for (A) POPS$_4$/E71H/KWK, (B) POPS/E71H/KWK, (C) POPC$_4$/E71H/KWK and (D) POPC/E71H/KWK from umbrella sampling simulations. The ion configurations are shown in a simplified representation of the selectivity filter. K$^+$ ions and water molecules are displayed as red and blue spheres, respectively. It should be noted that four ions are tracked in all cases but are not shown in the configuration when they are distant from the selectivity filter.

KK Mechanism

An alternative mechanism of conduction has also been proposed, excluding the involvement of water molecules [21]. In this mechanism, the selectivity filter contains two or three K$^+$ ions simultaneously, whilst the remaining sites are vacant, and direct ion-ion repulsion is responsible for low-energy conduction. The PMF for the KK mechanism can be found in Figure 4A-D. In POPS$_4$/E71H/KK and POPC$_4$/E71H/KK simulations, the energetic costs of ion exit to the extracellular solution (transitions I → II and II → III) and entrance from the

10

central cavity (transition III → IV) are between 2-4 kcal/mol. After this point, the computed barriers are of the order of 1 kcal/mol. In comparison to POPC$_4$/E71H/KK, the barriers reported for POPC/E71H/KK increase by between 1-1.5 kcal/mol. Similar to the KWK simulations, this is attributed to the preference of the S1 ion to bind centrally, increasing the energy required to leave S1 (transitions I → II and II → III) and pass through S1$_B$ (transition III → IV). Also related to this observation, configurations V (S1/S3/S4$_B$), VI (S1/S3/S4) and VII (S1/S2/S4) merge into a single minimum.

Table 3. Energetic barriers (>2 kcal/mol) calculated from umbrella sampling simulations for the KK mechanism with residues E71 protonated (E71H).

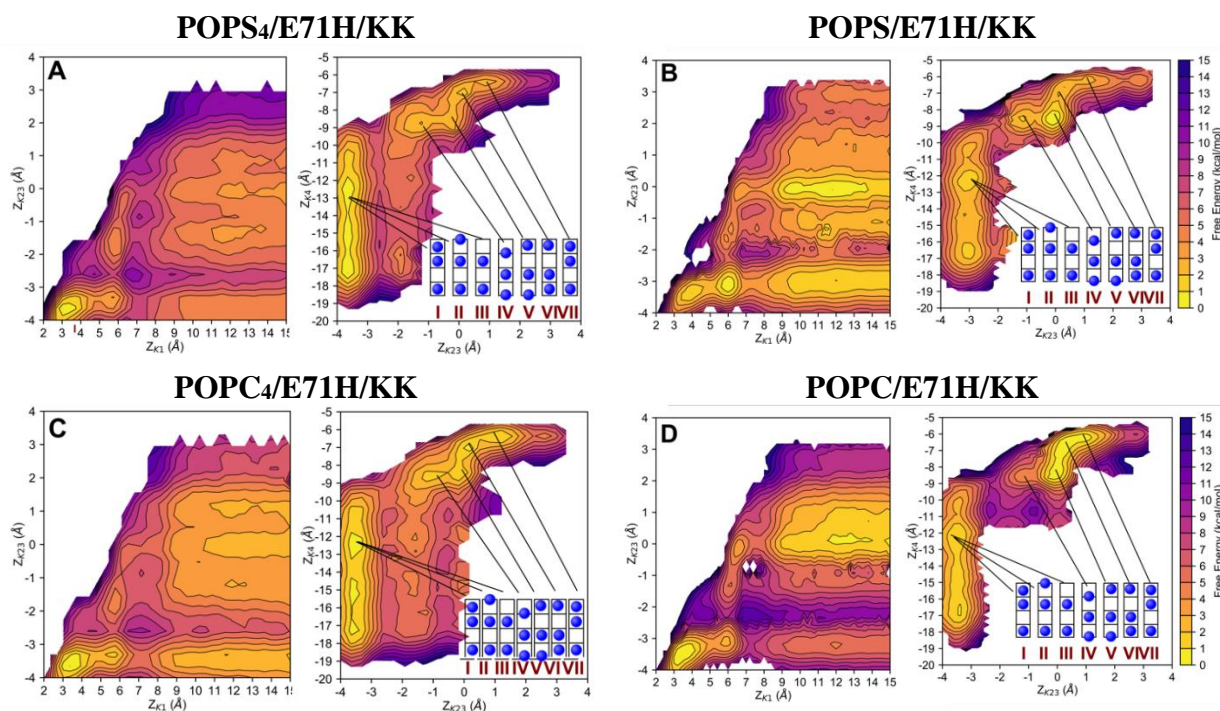| Simulation	Energy Barrier (kcal/mol ± SD)		
	I → II	II → III	III → IV
POPS$_4$/E71H/KK	3.8 ± 0.3	4.0 ± 0.5	3.0 ± 0.9
POPS/E71H/KK	1.6 ± 0.7	3.5 ± 0.5	4.1 ± 0.5
POPC$_4$/E71H/KK	2.3 ± 0.2	4.1 ± 0.5	3.7 ± 0.9
POPC/E71H/KK	3.6 ± 0.5	5.0 ± 0.5	5.2 ± 0.8

Figure 4. PMF profiles for (A) POPS$_4$/E71H/KK, (B) POPS/E71H/KK, (C) POPC$_4$/E71H/KK and (D) POPC/E71H/KK from umbrella sampling simulations. The ion configurations are shown in a simplified representation of the selectivity filter. K$^+$ ions and water molecules are displayed as red and blue spheres, respectively. It should be noted that four ions are tracked in all cases but are not shown in the configuration when they are distant from the selectivity filter.

Comparison of KWK and KK simulations

The maximum barrier to conduction is lowest in the POPS$_4$/E71H/KK and POPC$_4$/E71H/KK simulations (<~4 kcal/mol) suggesting the presence of non-annular lipids (both zwitterionic and anionic) and absence of water molecules from the selectivity filter are the most favorable conditions for conduction. Similar energies are observed during the KK mechanism when POPS is present in the membrane, but not in the non-annular sites (POPS/E71H/KK). In both conduction mechanisms, the highest barriers are observed in POPC/E71H simulations. In this scenario, the average RMSD of the selectivity filter residues in the umbrella sampling simulations is higher (Table 4). It should be noted that only windows common throughout the KWK or KK sets of simulations were included, therefore effects resulting from the position of ions can be considered negligible. The increased RMSD can be attributed to the interaction between non-annular arginine R89 and D80. In POPC/E71H simulations, the R89-D80 interaction is stable in three out four subunits. Instead, this interaction is observed in only 1 out of 4 subunits in POPS/E71H, and it is absent in POPS$_4$/E71H and POPC$_4$/E71H simulations. Further to this, the presence of the D80-R89 interaction, is associated with side-chain rotation of E71 to a X$_1$ dihedral in the range 160 to -160º (Table 4), The X$_1$ dihedral is typically in the range 40 to 100º, consistent with the crystal structure (60º), or it can spontaneously flip to occupy a conformation -50 to -80º in a single subunit in each simulation. It can be speculated that the deviation of the E71 sidechain contributes to the altered PMF profiles.

Table 4. Structural features of the KcsA selectivity filter in the umbrella sampling simulations. The RMSD of residues E71 to D80 is measured relative to the starting structure. The X$_1$ dihedral is measured as N-CA-CB-CG in the initial structure used for the simulation in individual subunits, denoted A-D. Subunits where the D80-R89 interaction is formed are denoted with an asterisk.

Simulation	Average RMSD (Å) ± SD		X$_1$ Dihedral (º)			
	KWK	**KK**	**A**	**B**	**C**	**D**
POPS$_4$/E71H	0.58 ± 0.07	0.50 ± 0.08	-78	53	76	101
POPS/E71H	0.68 ± 0.06	0.63 ± 0.07	-77	49	165*	73
POPC$_4$/E71H	0.65 ± 0.07	0.58 ± 0.07	67	67	80	-55
POPC/E71H	0.74 ± 0.06	0.68 ± 0.05	-70	84*	170*	-171*

E71 Deprotonated and KWK Simulations

When considering POPS$_4$/E71H/KWK *vs.* POPS$_4$/E71/KWK, negligible differences are observed in the calculated energetic barriers (Tables 2 and 5 and Figure 5). In contrast, the maximum barrier is reduced in POPC$_4$/E71/KWK (transitions III → IV: 2.0 ± 1.0 kcal/mol), in comparison to POPC$_4$/E71H/KWK (transitions III → IV: 5.5 ± 0.9 kcal/mol). This can be

attributed to the central position of the S1 ion in POPC$_4$/E71/KWK, in contrast to the alternate S1$_B$ site in POPC$_4$/E71H/KWK. This can be easily rationalized by considering the altered orientation and charge of E71. When protonated, the conformation of E71 is locked by coexistent hydrogen bonds with Y78 and D80, which in turn hydrogen bonds with W67. When deprotonated, the aforementioned hydrogen bond network is ruptured; instead, negatively charged E71 is oriented between the amide groups of G77 and Y78. In POPS$_4$/E71/KWK, the E71-Y78 hydrogen bond can be maintained, even though D80 is detached, resulting in the entire S1 site being hospitable and with negligible differences in energies in comparison to the protonated state (POPS$_4$/E71H/KWK). Therefore, it can be surmised that the rotation of the E71 side tampers with the energetics of the S1 site.

Table 5. Energetic barriers (>2 kcal/mol) calculated from umbrella sampling simulations for the KWK mechanism with residues E71 deprotonated.

Simulation	Energy Barrier (kcal/mol ± SD)		
	I → II	II → III	III → IV
POPS$_4$/E71/KWK	3.4 ± 0.9	2.7 ± 0.9	5.2 ± 1.0
POPC$_4$/E71/KWK	3.0 ± 0.8	3.0 ± 0.3	2.0 ± 1.0

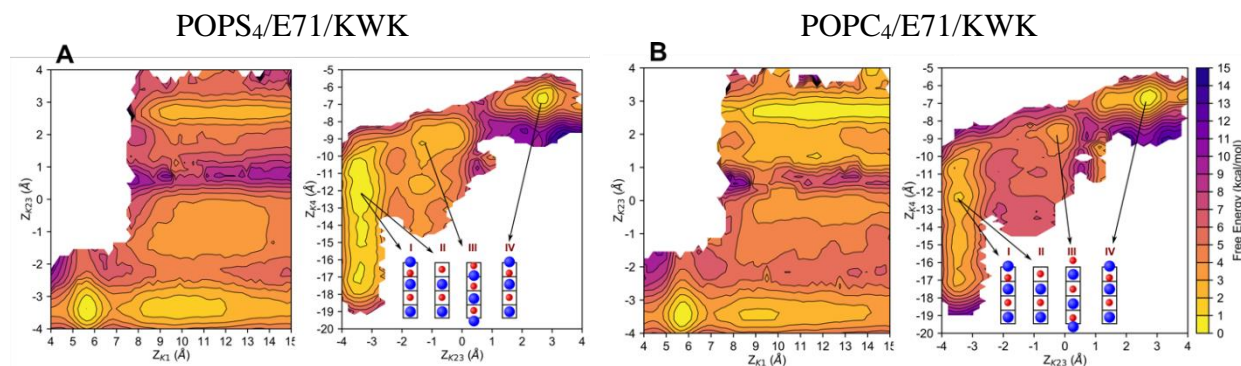POPS$_4$/E71/KWK   POPC$_4$/E71/KWK

Figure 5. PMF profiles for (A) POPS$_4$/E71/KWK and (B) POPC$_4$/E71/KWK from umbrella sampling simulations. The ion configurations are shown in a simplified representation of the selectivity filter. K$^+$ ions and water molecules are displayed as red and blue spheres, respectively. It should be noted that four ions are tracked in all cases but are not shown in the configuration when they are distant from the selectivity filter.

E71 Deprotonated and KK Simulations

In this conduction mechanism, the exact sequence of movements during ion translocation diverges when the protonation state of E71 is modified (Figure 6). When E71 is deprotonated (POPS$_4$/E71/KK and POPC$_4$/E71/KK), a configuration involving ions in the adjacent S2/S3 sites emerges (configurations II and III in Figure 6), which is absent when E71 is protonated.

This is likely because the heightened negative charge density in this region increases the tendency of positively charged ions to enter such conformations in the absence of water. The PMF profiles are considered in 4D to account for the additional configurations. The maximum barrier to conduction in both cases is ~5 kcal/mol (Table 6); this is a slight increase from the ~4 kcal/mol barrier in POPS$_4$/E71H/KK and POPC$_4$/E71H/KK simulations. As negligible differences are observed when comparing POPS$_4$/E71/KK and POPC$_4$/E71/KK, it can be suggested that the elevated charge density behind the selectivity filter is responsible for altering the energetics of different ion configurations, rather than the variable H-bonding attributes of E71, as mentioned for the KWK mechanism.

Table 6. Energetic barriers (>2 kcal/mol) calculated from umbrella sampling simulations for the KK mechanism with residues E71 deprotonated.

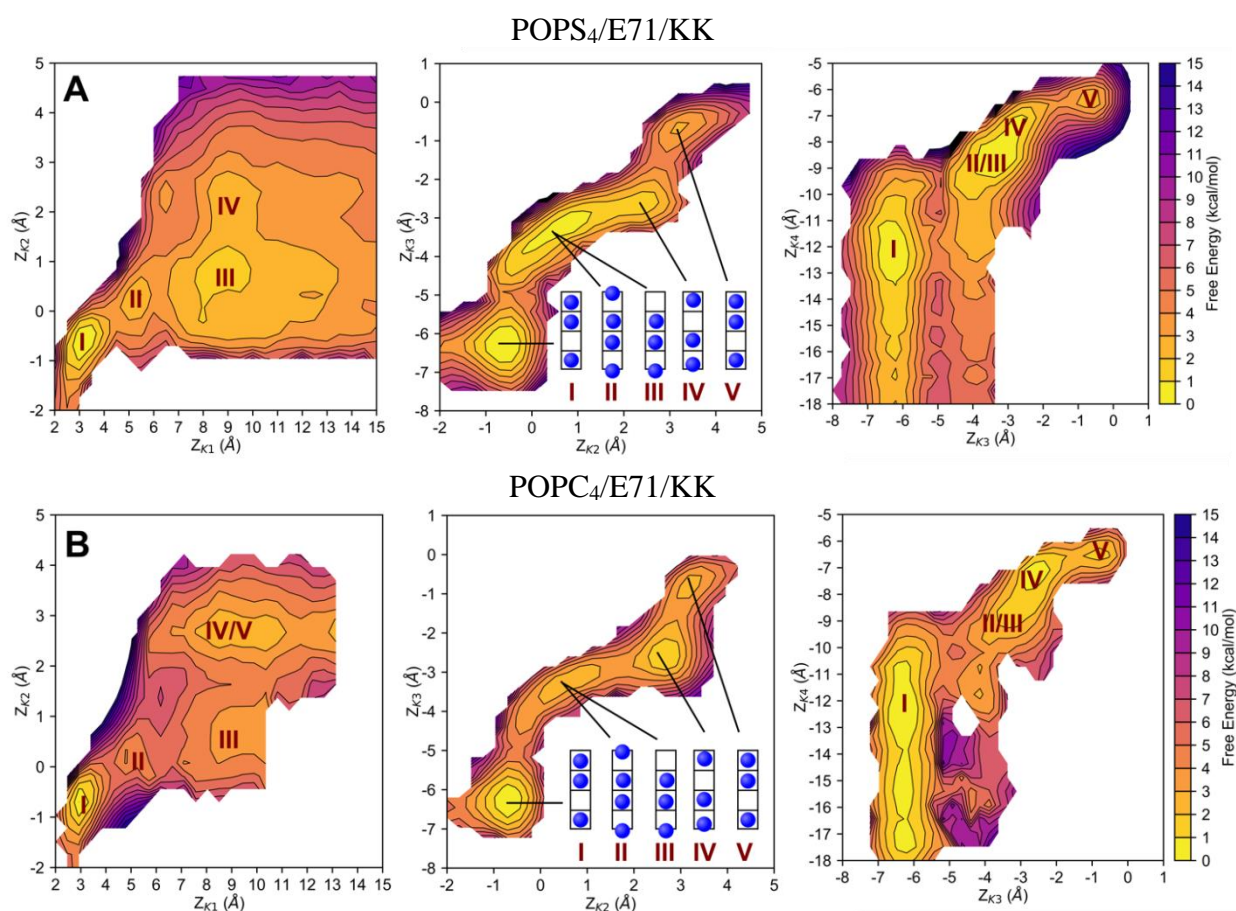| Simulation	Energy Barrier (kcal/mol ± SD)	
	I → II	IV → V
POPS$_4$/E71/KK	4.6 ± 0.6	2.8 ± 0.2
POPC$_4$/E71/KK	5.2 ± 0.8	< 2

Figure 6. PMF profiles for (A) POPS$_4$/E71/KK and (B) POPC$_4$/E71/KK from umbrella sampling simulations. The ion configurations are shown in a simplified representation of the selectivity filter. K$^+$ ions and water molecules are displayed as red and blue spheres,

respectively. It should be noted that four ions are tracked in all cases but are not shown in the configuration when they are distant from the selectivity filter.

Discussion

The umbrella sampling technique is an established method to characterize PMF of ion transport across the KcsA selectivity filter [55]. In several studies, the maximum energy barrier for the KWK mechanism has been calculated to be in the range between 2-3 kcal/mol [15, 16, 21]. However, a recent study utilizing the same closed KcsA structure has reported larger energy barriers of approximately 6 kcal/mol, corresponding to the transition between S1/S3/S4$_B$ and S0/S2/S4 configuration [56], similar to the PMFs presented in this study. By comparison with an artificial open-state structure formed from combination of an open-state structure and the closed-state selectivity filter, the authors of this study advocate that opening of the intracellular gate enable greater fluctuations in the selectivity filter, transforming the selectivity filter from a prohibitive closed state to a permissible open state [56]. Our results show that several pathways exist where ions can traverse the selectivity filter in the closed-state structure (PDB 1K4C: used in both studies) [31] with energies around 5 kcal/mol or less (POPS$_4$/E71H/KWK, POPS$_4$/E71H/KK, POPS/E71H/KK and POPC$_4$/E71H/KK). Overall, the maximum barrier to conduction is reported to be between 4.0 ± 0.5 and 6.7 ± 0.9 kcal/mol, considering all the situations presented where E71 is protonated. Remarkably, the lowest barrier calculated overall is observed for POPC$_4$/E71/KWK (3.0 ± 0.8 kcal/mol), suggesting ions can feasibly traverse the selectivity filter when E71 is deprotonated.

Comparison of the PMF profiles of conduction in zwitterionic and zwitterionic/anionic lipid bilayers, in the presence and absence of non-annular lipids reveals several important conclusions. Bearing in mind the fact that the free energy surfaces presented in this study are obtained in the period of POPC or POPS binding respectively with no exchange, somewhat surprisingly, differences in membrane composition can have a negligible impact to the maximum barrier to conduction, in the canonical structure of the selectivity filter. However, both non-annular lipids and the orientation of E71 can tune the occupancy of individual binding sites in the selectivity filter. This is significant considering that individual sites in K$^+$-channel selectivity filter have previously been shown to be critical for K$^+$ selectivity [57], maintaining the structural stability of the filter [58], and regulating both the rate of inactivation and recovery from it [55].

Several lines of inquiry have been investigated previously to fathom how the K$^+$ selectivity filter inactivates. Increasing the concentration of the permeant ion (K$^+$) or substitution of K$^+$

with Rb^{+} has been shown to decrease the rate of C-type inactivation [59, 60] and alter the ion occupancy at particular binding sites at the filter [61, 62], indicating a relationship between the two factors may exist [63, 64]. Considering this, it has been proposed that ion binding at a specific site prevents inactivation from occurring [59, 65]. The S2 site has been implicated in this mechanism in several studies [66, 67]. In opposition to this, Matulef and coworkers propose that the lack of ion binding in S2 reduces inactivation [68]. In this study, KcsA amide-to-ester (G77-ester, Y78-ester and G79-ester) substitutions are shown to reduce the single-channel conductance relative to wild type KcsA, in a similar manner. Y78-ester and G77-ester mutations also significantly reduce inactivation, relative to wild type KcsA and G79-ester mutant. The amide-ester mutation adjusts the H-bonding and electrostatic properties of the residue; quantitively, the electronegativity on the carbonyl oxygen is approximately halved in the ester [69]. The crystal structure of the Y78-ester, resolved in the same publication, reveals that these properties eliminate ion binding at S2. The ion occupancy is considered to be the major contributing factor to inactivation, considering the S2 ion occupancy is also lessened in the Rb^{+} wild type structure, relative to the K^{+} wild type, yet the H-bond interactions are maintained.

The noted structural and functional properties of the Y78-ester mutant, and the PMF profiles presented in this study, lead us to propose through what medium membrane lipids modulate inactivation of KcsA by facilitating or preventing networks of interactions with key residues. In the PMF profiles, the energetics of the $S1_B$ site, which is equivalent to the Y78 carbonyl oxygen above the S2 site, are divergent throughout. For example, in POPC/E71H/KWK and POPC/E71H/KK configurations involving S1 occupation are noticeably lower in energy than those involving $S1_B$, in contrast to other simulations (POPC$_4$/E71H, POPS$_4$/E71H, POPS/E71H, KWK or KK), where configurations involving S1 and $S1_B$ are roughly equivalent or $S1_B$ configurations are lower in energy than the $S1/S3/S4_B$ configuration. The absence of an energy minima in the plane of the four Y78-carbonyl oxygen atoms ($S1_B$) in POPC/E71H/KWK and POPC/E71H/KK is significant considering the observed interactions between R89 (an arginine residue in the non-annular sites) and D80 in three out of four subunits, and the side-chain rotation of E71 in those subunits, which is absent elsewhere. The D80-R89 interaction has been reported previously [28]. With this in mind, we hypothesize that membrane lipids modulate the conformation and interactions of residues surrounding the selectivity filter, which biases the occupancy of individual selectivity filter sites and regulates

the inactivation process. Further experimental and simulation studies will be required to examine this theory in detail.

Conclusions

There have been an increasing number of studies illustrating the importance of protein-lipid interactions in the context of structures and the stability of K^+-channels [70]. Ion conduction in K^+-channels is regulated at the lower helix-bundle crossing gate that may be mechanically coupled to other regulatory domains. Besides, the lower helix-bundle is in many cases functionally coupled to the opening or closing of the selectivity filter gate. In KcsA, the inner gate is destabilized at acidic pH shifting the equilibrium toward its open conformation. In contrast, the outer gate at the selectivity filter defines primarily the channel opening probability and fluctuates between an open state and a non-permeation state, a process known as inactivation. In this context, the function of K^+-channels, and in particular KcsA, has been shown to be regulated by membrane lipids [22, 71]. High-resolution structural information available for KcsA reveals that it contains non-covalently bound lipid identified as phosphatidylglycerol (PG) [4, 6, 22, 24, 26-28]. We have previously showed that the presence of 1-palmitoyl-2-oleoyl phosphatidic acid (POPA) drastically reduces inactivation in macroscopic current recordings. Effects akin to those of POPA on wild type KcsA were observed when either one or both R64 and R89 were mutated to alanine in the absence of added anionic lipids. These results were interpreted as a consequence of the interactions between the arginine residues and the anionic POPA molecules bound to the non-annular sites [29].

In this study, umbrella sampling simulations have been used to compute the energetics of ion permeation through the KcsA selectivity filter, via two mechanisms of conduction involving either water or vacant sites. The effect of membrane composition, specifically anionic lipids, and E71 protonation state are assessed, serving as contemporary aspects of this work. The information gained brings to light several novel prospects concerning the behaviour of the KcsA selectivity filter: (i) anionic lipids do not affect the energetic barriers of K^+ through the canonical selectivity filter structure, (ii) selectivity filter conformations involving the deprotonated E71 residue are associated with similar energetic barriers, and (iii) the occupancies of individual selectivity filter sites are affected by the presence and identity of non-annular lipids. The latter observation has been discussed in the context of KcsA inactivation, and a mechanism which might explain the known relationship between membrane composition and inactivation rate has been proposed. This hypothesis can be used as a starting point for future studies.

REFERENCES

[1] A. Rosenhouse-Dantsker, D. Mehta, I. Levitan, Regulation of Ion Channels by Membrane Lipids, Comprehensive Physiology, 2 (2012) 31-68.

[2] I. Levitan, D.K. Singh, A. Rosenhouse-Dantsker, Cholesterol binding to ion channels, Frontiers in Physiology, 5 (2014) 14.

[3] F.C. Coyan, G. Loussouarn, Cholesterol regulation of ion channels: Crosstalk in proteins, crosstalk in lipids, Channels, 7 (2013) 415-416.

[4] S.S. Deol, C. Domene, P.J. Bond, M.S.P. Sansom, Anionic phospholipid interactions with the potassium channel KcsA: Simulation studies, Biophysical Journal, 90 (2006) 822-830.

[5] C. Domene, P.J. Bond, S.S. Deol, M.S.P. Sansom, Lipid/protein interactions and the membrane/water interfacial region, Journal of the American Chemical Society, 125 (2003) 14966-14967.

[6] P. Marius, M. Zagnoni, M.E. Sandison, J.M. East, H. Morgan, A.G. Lee, Binding of anionic lipids to at least three nonannular sites on the potassium channel KcsA is required for channel opening, Biophysical Journal, 94 (2008) 1689-1698.

[7] M. Iwamoto, S. Oiki, Amphipathic antenna of an inward rectifier K+ channel responds to changes in the inner membrane leaflet, Proceedings of the National Academy of Sciences of the United States of America, 110 (2013) 749-754.

[8] M. Raja, R.E.J. Spelbrink, B. de Kruijff, J.A. Killian, Phosphatidic acid plays a special role in stabilizing and folding of the tetrameric potassium channel KcsA, Febs Letters, 581 (2007) 5715-5722.

[9] M. Raja, The Role of Extramembranous Cytoplasmic Termini in Assembly and Stability of the Tetrameric K+-Channel KcsA, Journal of Membrane Biology, 235 (2010) 51-61.

[10] I. Triano, F.N. Barrera, M.L. Renart, M.L. Molina, G. Fernandez-Ballester, J.A. Poveda, A.M. Fernandez, J.A. Encinar, A.V. Ferrer-Montiel, D. Otzen, J.M. Gonzalez-Ros, Occupancy of Nonannular Lipid Binding Sites on KcsA Greatly Increases the Stability of the Tetrameric Protein, Biochemistry, 49 (2010) 5397-5404.

[11] F.N. Barrera, M.L. Renart, J.A. Poveda, B. De Kruijff, J.A. Killian, J.M. Gonzalez-Ros, Protein self-assembly and lipid binding in the folding of the potassium channel KcsA, Biochemistry, 47 (2008) 2123-2133.

[12] D.A. Doyle, J.M. Cabral, R.A. Pfuetzner, A.L. Kuo, J.M. Gulbis, S.L. Cohen, B.T. Chait, R. MacKinnon, The structure of the potassium channel: Molecular basis of K+ conduction and selectivity, Science, 280 (1998) 69-77.

[13] O.S. Smart, J.M. Goodfellow, B.A. Wallace, The pore dimensions of gramicidin A, Biophysical Journal, 65 (1993) 2455-2460.

[14] L. Heginbotham, Z. Lu, T. Abramson, R. MacKinnon, Mutations in the K+ channel signature sequence, Biophysical Journal, 66 (1994) 1061-1067.

[15] J. Aqvist, V. Luzhkov, Ion permeation mechanism of the potassium channel, Nature, 404 (2000) 881-884.

[16] S. Berneche, B. Roux, Energetics of ion conduction through the K+ channel, Nature, 414 (2001) 73-77.

[17] C. Domene, S. Furini, On ionic conduction in potassium channels, Proceedings of the National Academy of Sciences of the United States of America, 107 (2010) 14938-14938.

[18] H. Bernsteiner, E.-M. Zangerl-Plessl, X. Chen, A. Stary-Weinzinger, Conduction through a narrow inward-rectifier K+ channel pore, Journal of General Physiology, 151 (2019) 1231-1246.

[19] T. Sumikama, S. Oiki, Digitalized K+ Occupancy in the Nanocavity Holds and Releases Queues of K+ in a Channel, Journal of the American Chemical Society, 138 (2016) 10284-10292.

[20] C. Domene, M.S. Sansom, Potassium channel, ions, and water: simulation studies based on the high resolution X-ray structure of KcsA, Biophys J, 85 (2003) 2787-2800.

[21] Furini, C. Domene, Atypical mechanism of conduction in potassium channels, Proc Natl Acad Sci U S A, 106 (2009) 16074-16077.

[22] F.I. Valiyaveetil, Y. Zhou, R. MacKinnon, Lipids in the Structure, Folding, and Function of the KcsA K+ Channel, Biochemistry, 41 (2002) 10771-10777.

[23] Zhou, Morais-Cabral, Kaufman, MacKinnon, Chemistry of ion coordination and hydration revealed by a K+ channel-Fab complex at 2.0 angstrom resolution, Nature, 414 (2001) 43-48.

[24] J.A.A. Demmers, A. van Dalen, B. de Kruijff, A.J.R. Heck, J.A. Killian, Interaction of the K+ channel KcsA with membrane phospholipids as studied by ESI mass spectrometry, Febs Letters, 541 (2003) 28-32.

[25] A.G. Lee, How lipids affect the activities of integral membrane proteins, Biochimica Et Biophysica Acta-Biomembranes, 1666 (2004) 62-87.

[26] P. Marius, S.J. Alvis, J.M. East, A.G. Lee, The interfacial lipid binding site on the potassium channel KcsA is specific for anionic phospholipids, Biophysical Journal, 89 (2005) 4081-4089.

[27] P. Marius, M.R.R. de Planque, P.T.F. Williamson, Probing the interaction of lipids with the non-annular binding sites of the potassium channel KcsA by magic-angle spinning NMR, Biochimica Et Biophysica Acta-Biomembranes, 1818 (2012) 90-96.

[28] M. Weingarth, A. Prokofyev, E.A.W. van der Cruijsen, D. Nand, A. Bonvin, O. Pongs, M. Baldus, Structural Determinants of Specific Lipid Binding to Potassium Channels, Journal of the American Chemical Society, 135 (2013) 3983-3988.

[29] J.A. Poveda, A.M. Giudici, M.L. Renart, O. Millet, A. Morales, J.M. González-Ros, V. Oakes, S. Furini, C. Domene, Modulation of the potassium channel KcsA by anionic phospholipids: Role of arginines at the non-annular lipid binding sites, Biochimica et Biophysica Acta (BBA) - Biomembranes, 1861 (2019) 183029.

[30] M.L. Molina, J.A. Encinar, F.N. Barrera, G. Fernandez-Ballester, G. Riquelme, J.M. Gonzalez-Ros, Influence of C-terminal protein domains and protein-lipid interactions on tetramerization and stability of the potassium channel KcsA, Biochemistry, 43 (2004) 14924-14931.

[31] Y.F. Zhou, J.H. Morais-Cabral, A. Kaufman, R. MacKinnon, Chemistry of ion coordination and hydration revealed by a K+ channel-Fab complex at 2.0 angstrom resolution, Nature, 414 (2001) 43-48.

[32] S. Berneche, B. Roux, The ionization state and the conformation of Glu-71 in the KcsA K+ channel, Biophysical Journal, 82 (2002) 772-780.

[33] S. Jo, T. Kim, V.G. Iyer, W. Im, CHARMM-GUI: a web-based graphical user interface for CHARMM, Journal of computational chemistry, 29 (2008) 1859-1865.

[34] S. Jo, J.B. Lim, J.B. Klauda, W. Im, CHARMM-GUI Membrane Builder for Mixed Bilayers and Its Application to Yeast Membranes, Biophysical Journal, 97 (2009) 50-58.

[35] E.L. Wu, X. Cheng, S. Jo, H. Rui, K.C. Song, E.M. Dávila-Contreras, Y. Qi, J. Lee, V. Monje-Galvan, R.M. Venable, CHARMM-GUI Membrane Builder toward realistic biological membrane simulations, Journal of computational chemistry, 35 (2014) 1997-2004.

[36] W. Humphrey, A. Dalke, K. Schulten, VMD: Visual molecular dynamics, Journal of Molecular Graphics, 14 (1996) 33-38.

[37] J.C. Phillips, R. Braun, W. Wang, J. Gumbart, E. Tajkhorshid, E. Villa, C. Chipot, R.D. Skeel, L. Kale, K. Schulten, Scalable molecular dynamics with NAMD, Journal of computational chemistry, 26 (2005) 1781-1802.

[38] J.B. Klauda, R.M. Venable, J.A. Freites, J.W. O'Connor, D.J. Tobias, C. Mondragon-Ramirez, I. Vorobyov, A.D. MacKerell Jr, R.W. Pastor, Update of the CHARMM all-atom additive force field for lipids: validation on six lipid types, The journal of physical chemistry B, 114 (2010) 7830-7843.

[39] W.L. Jorgensen, J. Chandrasekhar, J.D. Madura, R.W. Impey, M.L. Klein, Comparison of simple potential functions for simulating liquid water, The Journal of chemical physics, 79 (1983) 926-935.

[40] B. Roux, S. Berneche, On the potential functions used in molecular dynamics simulations of ion channels, Biophysical Journal, 82 (2002) 1681-1684.

[41] T. Darden, D. York, L. Pedersen, Particle mesh Ewald: An N·log(N) method for Ewald sums in large systems, The Journal of chemical physics, 98 (1993) 10089-10092.

[42] S. Miyamoto, P.A. Kollman, SETTLE: an analytical version of the SHAKE and RATTLE algorithm for rigid water models, J. Comput. Chem., 13 (1992) 952-962.

[43] S.E. Feller, Y. Zhang, R.W. Pastor, B.R. Brooks, Constant pressure molecular dynamics simulation: the Langevin piston method, The Journal of chemical physics, 103 (1995) 4613-4621.

[44] G.J. Martyna, D.J. Tobias, M.L. Klein, Constant pressure molecular dynamics algorithms, The Journal of Chemical Physics, 101 (1994) 4177-4189.

[45] S. Furini, C. Domene, Selectivity and permeation of alkali metal ions in K+-channels, J Mol Biol, 409 (2011) 867-878.

[46] S. Furini, C. Domene, Nonselective Conduction in a Mutated NaK Channel with Three Cation-Binding Sites, Biophysical Journal, 103 (2012) 2106-2114.

[47] S. Furini, C. Domene, K(+) and Na(+) Conduction in Selective and Nonselective Ion Channels Via Molecular Dynamics Simulations, Biophysical Journal, 105 (2013) 1737-1745.

[48] S. Kumar, D. Bouzida, R.H. Swendsen, P.A. Kollman, J.M. Rosenberg, The weighted histogram analysis method for free-energy calculations on biomolecules. 1. Method., Journal of computational chemistry, 13 (1992) 1011-1021.

[49] E. Weinan, W.Q. Ren, E. Vanden-Eijnden, String method for the study of rare events, Phys Rev B, 66 (2002).

[50] Y. Jiang, A. Lee, J. Chen, M. Cadene, B.T. Chait, R. MacKinnon, The open pore conformation of potassium channels, Nature, 417 (2002) 523-526.

[51] C. Domene, S. Vemparala, S. Furini, K. Sharp, M.L. Klein, The role of conformation in ion permeation in a K+ channel, J Am Chem Soc, 130 (2008) 3389-3398.

[52] C. Miller, COUPLING OF WATER AND ION FLUXES IN A K+-SELECTIVE CHANNEL OF SARCOPLASMIC-RETICULUM, Biophysical Journal, 38 (1982) 227-230.

[53] C. Alcayaga, X. Cecchi, O. Alvarez, R. Latorre, STREAMING POTENTIAL MEASUREMENTS IN CA-2+-ACTIVATED K+ CHANNELS FROM SKELETAL AND SMOOTH-MUSCLE - COUPLING OF ION AND WATER FLUXES, Biophysical Journal, 55 (1989) 367-371.

[54] H.T. Kratochvil, J.K. Carr, K. Matulef, A.W. Annen, H. Li, M. Maj, J. Ostmeyer, A.L. Serrano, H. Raghuraman, S.D. Moran, J.L. Skinner, E. Perozo, B. Roux, F.I. Valiyaveetil, M.T. Zanni, Instantaneous ion configurations in the K+ ion channel selectivity filter revealed by 2D IR spectroscopy, Science, 353 (2016) 1040-1044.

[55] C. Domene, S. Furini, Examining ion channel properties using free-energy methods, in: M.L. Johnson, J.M. Holt, G.K. Ackers (Eds.) Methods in Enzymology, Vol 466: Biothermodynamics, Pt B, vol. 466, 2009, pp. 155-+.

[56] F.T. Heer, D.J. Posson, W. Wojtas-Niziurski, C.M. Nimigean, S. Berneche, Mechanism of activation at the selectivity filter of the KcsA K+ channel, Elife, 6 (2017) 18.

[57] C. Domene, S. Furini, Dynamics, energetics, and selectivity of the low-K+ KcsA channel structure, J Mol Biol, 389 (2009) 637-645.

[58] S. Furini, C. Domene, Gating at the selectivity filter of ion channels that conduct Na+ and K+ ions, Biophys J, 101 (2011) 1623-1631.

[59] J. Lopezbarneo, T. Hoshi, S.H. Heinemann, R.W. Aldrich, Effects of External Cations and Mutations in the Pore Region on C-Type Inactivation of Shaker Potassium Channels, Receptors & channels, 1 (1993) 61-71.

[60] L. Kiss, S.J. Korn, Modulation of C-type inactivation by K+ at the potassium channel selectivity filter, Biophysical Journal, 74 (1998) 1840-1849.

[61] J.H. Morais-Cabral, Y.F. Zhou, R. MacKinnon, Energetic optimization of ion conduction rate by the K+ selectivity filter, Nature, 414 (2001) 37-42.

[62] Y.F. Zhou, R. MacKinnon, The occupancy of ions in the K+ selectivity filter: Charge balance and coupling of ion binding to a protein conformational change underlie high conduction rates, Journal of Molecular Biology, 333 (2003) 965-975.

[63] L. Kiss, J. LoTurco, S.J. Korn, Contribution of the selectivity filter to inactivation in potassium channels, Biophysical Journal, 76 (1999) 253-263.

[64] E.M. Ogielska, R.W. Aldrich, Functional consequences of a decreased potassium affinity in a potassium channel pore - Ion interactions and C-type inactivation, Journal of General Physiology, 113 (1999) 347-358.

[65] T. Baukrowitz, G. Yellen, MODULATION OF K+ CURRENT BY FREQUENCY AND EXTERNAL K+ - A TALE OF 2 INACTIVATION MECHANISMS, Neuron, 15 (1995) 951-960.

[66] L.G. Cuello, V. Jogini, D.M. Cortes, E. Perozo, Structural mechanism of C-type inactivation in K+ channels, Nature, 466 (2010) 203-U273.

[67] D.M. Cortes, L.G. Cuello, E. Perozo, Molecular architecture of full-length KcsA - Role of cytoplasmic domains in ion permeation and activation gating, Journal of General Physiology, 117 (2001) 165-180.

[68] K. Matulef, A.G. Komarov, C.A. Costantino, F.I. Valiyaveetil, Using protein backbone mutagenesis to dissect the link between ion occupancy and C-type inactivation in K+ channels, Proceedings of the National Academy of Sciences of the United States of America, 110 (2013) 17886-17891.

[69] E.T. Powers, S. Deechongkit, J.W. Kelly, BACKBONE-BACKBONE H-BONDS MAKE CONTEXT-DEPENDENT CONTRIBUTIONS TO PROTEIN FOLDING KINETICS AND THERMODYNAMICS: LESSONS FROM AMIDE-TO-ESTER MUTATIONS, Peptide Solvation and H-Bonds, 72 (2005) 39-78.

[70] K.M. Callahan, B. Mondou, L. Sasseville, J.-L. Schwartz, N. D'Avanzo, The influence of membrane bilayer thickness on KcsA channel activity, Channels, 13 (2019) 424-439.

[71] M.L. Molina, A.M. Giudici, J.A. Poveda, G. Fernández-Ballester, E. Montoya, M.L. Renart, A.M. Fernández, J.A. Encinar, G. Riquelme, A. Morales, J.M. González-Ros, Competing Lipid-Protein and Protein-Protein Interactions Determine Clustering and Gating Patterns in the Potassium Channel from Streptomyces lividans (KcsA), Journal of Biological Chemistry, 290 (2015) 25745-25755.